Cognitive Enhancement via Network-Targeted Cortico-cortical Associative Brain Stimulation

Article *in* Cerebral Cortex · October 2019

DOI: 10.1093/cercor/bhz182

10 authors, including:

Davide Momi
Università degli Studi G. d'Annunzio Chieti e Pescara
11 PUBLICATIONS **10** CITATIONS
SEE PROFILE

Francesco Neri
Brain Investigation and Neuromodulation laboratory, Department of Medicine, Su…
10 PUBLICATIONS **8** CITATIONS
SEE PROFILE

Domenica Veniero
University of Nottingham
64 PUBLICATIONS **1,178** CITATIONS
SEE PROFILE

Giulia Sprugnoli
Università di Parma
16 PUBLICATIONS **20** CITATIONS
SEE PROFILE

Cerebral Cortex, 2019;00: 1–12

doi: 10.1093/cercor/bhz182
Advance Access Publication Date: 00 Month 0000
Original Article

ORIGINAL ARTICLE

Cognitive Enhancement via Network-Targeted Cortico-cortical Associative Brain Stimulation

D. Momi[1], F. Neri[1], G. Coiro[1], C. Smeralda[1], D. Veniero[2], Sprugnoli G.[1], Rossi A.[1], Pascual-Leone A.[3], Rossi S.[1,4] and Santarnecchi E.[1,3]

[1]Brain Investigation and Neuromodulation Laboratory, Department of Medicine, Surgery and Neuroscience, Siena School of Medicine, 53100 Siena, Italy, [2]Institute of Neuroscience and Psychology, University of Glasgow, G12 8QQ Glasgow, UK, [3]Berenson-Allen Center for Noninvasive Brain Stimulation, Division of Cognitive Neurology, Department of Neurology, Beth Israel Deaconess Medical Center, Harvard Medical School, Boston, MA 02215, USA and [4]Human Physiology Section, Department of Medicine, Surgery and Neuroscience, University of Siena, 53100 Siena, Italy

Address correspondence to Emiliano Santarnecchi, Berenson-Allen Center for Noninvasive Brain Stimulation, Beth Israel Deaconess Medical Center, Harvard Medical School, Boston, MA 02215, USA. Email: esantarn@bidmc.harvard.edu

Abstract

Fluid intelligence (*gf*) represents a crucial component of human cognition, as it correlates with academic achievement, successful aging, and longevity. However, it has strong resilience against enhancement interventions, making the identification of *gf* enhancement approaches a key unmet goal of cognitive neuroscience. Here, we applied a spike-timing-dependent plasticity (STDP)-inducing brain stimulation protocol, named cortico-cortical paired associative stimulation (cc-PAS), to modulate *gf* in 29 healthy young subjects (13 females—mean ± standard deviation, 25.43 years ± 3.69), based on dual-coil transcranial magnetic stimulation (TMS). Pairs of neuronavigated TMS pulses (10-ms interval) were delivered over two frontoparietal nodes of the *gf* network, based on individual functional magnetic resonance imaging data and in accordance with cognitive models of information processing across the prefrontal and parietal lobe. cc-PAS enhanced accuracy at *gf* tasks, with parieto-frontal and fronto-parietal stimulation significantly increasing logical and relational reasoning, respectively. Results suggest the possibility of using SPTD-inducing TMS protocols to causally validate cognitive models by selectively engaging relevant networks and manipulating inter-regional temporal dynamics supporting specific cognitive functions.

Key words: abstract reasoning, fluid intelligence, Hebbian plasticity, logical reasoning, transcranial magnetic stimulation

Introduction

Daily scenarios constantly challenge our life with tasks requiring much more than a mere access to previously consolidated knowledge. The ability to extrapolate, filter, and organize new information constitutes a critical component of human cognition, commonly referred as fluid intelligence (*gf*) (Cattell 1963; Horn and Cattell 1966). Indeed, *gf* positively correlates with a vast number of cognitive abilities. It is an important predictor of socioeconomic status, longevity (Gottfredson and Deary 2004), academic and professional success (Neisser et al. 1996; Gottfredson 2002; Deary et al. 2007; Rohde and Thompson 2007; te Nijenhuis et al. 2007; Watkins et al. 2007; Ren et al. 2015), as well as a predictor of brain robustness to lesions (Santarnecchi et al. 2015). However, individual *gf* abilities are resilient to external

manipulation (Haier 2014), making the development of tools and methods for its enhancement a key unmet goal of contemporary cognitive neuroscience. Particularly, the possibility of increasing *gf* capacity might have relevant impact for both healthy and pathological brain functioning, potentially affecting learning abilities (Filicková et al. 2015), cognitive reserve (Stern 2002), and resilience processes (Santarnecchi et al. 2015).

Several attempts to increase *gf* have been made over the last two decades, based on a variety of interventions: cognitive training (Au et al. 2016), drugs (Stough et al. 2011), meditation (Gard et al. 2014), physical activity (Reed et al. 2010), videogames (Smith et al. 2013), diet (Beard et al. 2005), neurofeedback (Staufenbiel et al. 2014), musical training (Schellenberg 2004), as well as noninvasive brain stimulation (NIBS) (Pahor and Jaušovec 2014; Santarnecchi et al. 2016). Clearly, such interventions affect brain functioning in very different ways, ranging from rather focal (e.g., NIBS) to generalized (e.g., drugs, physical exercise, diet) effects, which might or might not be directly linked to the neurofunctional substrate of *gf*.

In the case of NIBS interventions, previous studies have been focused on transcranial alternating electrical stimulation of a single brain region applied in the gamma (i.e., 40 Hz) (Santarnecchi et al. 2013, 2016) or theta (i.e., 5 Hz) (Pahor and Jaušovec 2014; Neubauer et al. 2017) band, with enhancement observed during stimulation delivered over the left prefrontal and parietal regions, respectively. Transient increase in *gf* levels has also been observed after repetitive transcranial magnetic stimulation (TMS; 5 Hz) delivered over the left prefrontal cortex (Boroojerdi et al. 2001). Despite single region's activity has been recognized fundamental for *gf*-related processing, increasing evidence suggest the relevance of a distributed, bilateral frontoparietal brain network (for a review see Santarnecchi et al. 2017). Therefore, techniques allowing to manipulate such interplay with both high spatial and temporal specificity might represent the optimal approach to engage network dynamics underpinning *gf*.

In this regard, TMS offers the possibility of stimulating a small portion of cortical grey matter (i.e., $\sim 1\ cm^3$) with high spatial accuracy, especially when coupled with magnetic resonance imaging (MRI)-guided stereotaxic neuronavigation (Rossini and Rossi 2007). Repeatitive TMS protocols have been shown to lead to long-lasting changes in brain function (Guse et al. 2013). For instance, an increase in the expression of a potent modulator of synaptic plasticity (e.g., brain-derived neurotrophic factor, BDNF) has been reported after TMS (Müller et al. 2000).

When applied in the form of paired pulses delivered at predetermined intervals over two cortical regions (i.e., cortico-cortical paired associative stimulation—cc-PAS hereafter), TMS is thought of inducing spike-timing-dependent plasticity (STDP), by strengthening synaptic coupling between the two target neuronal populations (Stefan et al. 2000, 2002; Wolters et al. 2003). From a neurophysiological perspective, the interstimulus interval (ISI) represents the timing of interregional information transfer, that is, the time for the spikes induced by the first TMS pulse on Region A to reach neurons in Region B. When an appropriate ISI is chosen and stimulation is repeated over time (e.g., 200 pairs of pulses on A and B on the premotor and motor cortices), cc-PAS enhances A–B synaptic strength, leading to neurophysiologically measurable changes (e.g., increase of motor evoked potentials [MEPs], recorded from Region B) and a rearrangement of network-to-network dynamics (Santarnecchi et al. 2018). Importantly, the order of TMS pulses (A → B vs. B → A) has been shown to affect the direction of induced plasticity changes (Santarnecchi et al. 2018). Cc-PAS is therefore foreseen as a promising candidate for the modulation of cognitive processes, when specific cortical correlates are available and hypotheses about the direction of information processing can be drawn.

Based on such rationale, we tailored a cc-PAS protocol to modulate individual *gf* levels by inducing STDP between a network of brain regions responsible for *gf*-related problem solving (Fig. 1), aiming at increasing within-network connectivity. Participants performed a baseline visit in which functional magnetic resonance imaging (fMRI) and cognitive data were collected to guide subsequent stimulations and possibly identify predictors of response to cc-PAS (Fig. 1A). Specifically, the most positively correlated nodes of a recently published quantitative task-fMRI meta-analysis representing brain activity during *gf* problem solving (Santarnecchi et al. 2017) were identified for each participant and used as targets for neuro navigated double-coil TMS (Fig. 2).

We aimed to assess *gf* abilities at multiple time points before/after ccPAS, as well as investigate the impact of different cc-PAS conditions. Therefore, a *gf* task allowing for multiple, balanced parallel versions was used (Matzen et al. 2010). The (Sandia Matrices) task included both logical and relational problems, administered in a randomized order. Logical stimuli load mostly on prefrontal brain structures (Prado et al. 2010) and require the ability to solve problems such as "if P then Q" (operationalized in the Sandia task as, for example, "if there is a circle then there is a triangle. There is not a triangle. Therefore, there is not a circle.") Differently, relational problems engage mostly parietal activity (Prado et al. 2010) and require to make inference about riddles, such as "P is to the left of Q; Q is to the left of R" (operationalized in the Sandia task as "The circle is to the left of the triangle. The triangle is to the left of the square. Therefore, the circle is to the left of the square.") Besides such regional specificity of *gf*-related brain activity, a parietofrontal information processing gradient supports the solution of logical tasks (Houdé et al. 2000), while feedback projections from prefrontal to parietal regions support relational reasoning. By testing the impact of cc-PAS delivered following a parietofrontal (P → F, ISI = +10 ms) or a frontoparietal (F → P, ISI = −10 ms) associative direction, we designed a study possibly looking at direction-specific modulation of *gf* abilities (Fig. 1C). Additionally, control conditions investigating the effect of (1) nonassociative cc-PAS delivered simultaneously over frontal and parietal regions (i.e., Simultaneous-TMS, ISI = 0 ms) and (2) TMS targeting only the prefrontal lobe were also included (i.e., Prefrontal-TMS). Furthermore, to account for learning effects due to tasks repetition despite randomization of conditions, *gf* assessment was also tested (3) while participants received no stimulation, as a third control condition (i.e., no stimulation [NoStim], placebo "sham" TMS). Finally, control tasks addressing near (inhibition, via the Letter No-Go task [LNG]) and far (selective attention, via a visual search [VS] task) cognitive transfer were also administered before and after each stimulation session.

Overall, we aimed at testing the following hypotheses: (1) STDP-inducing cc-PAS protocols (i.e., P → F, F → P) will induce a change in *gf*-related cognitive performance as compared to nonassociative cc-PAS (Simultaneous-TMS), single region (Prefrontal-TMS), and NoStim conditions; (2) cc-PAS will affect *gf* performance depending on interregional stimulation direction, with a beneficial effect on logical reasoning for P → F TMS and on relational reasoning for F → P TMS, specifically. Finally, resting state fMRI data collected at baseline were used to predict

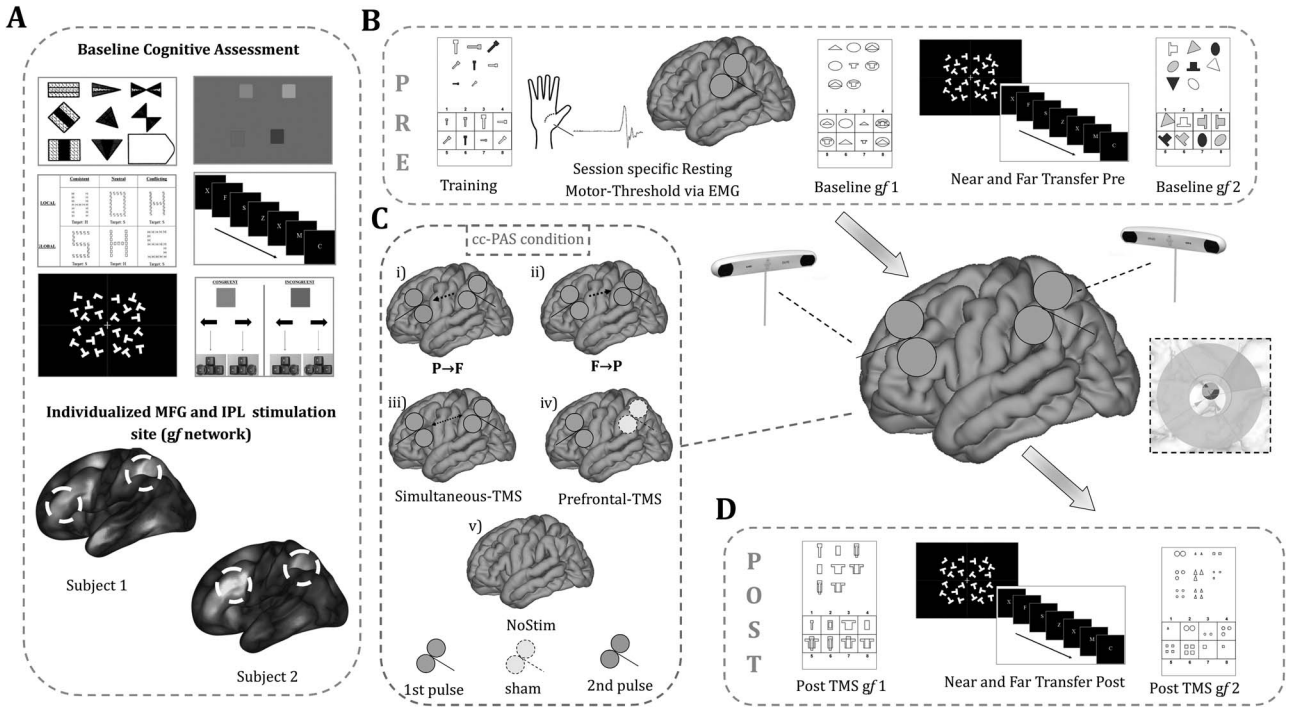

Figure 1. Experimental design. (*A*) Baseline assessment included a set of neuropsychological tests and resting state fMRI acquisition. A high degree of variability in functional connectivity of prefrontal and parietal TMS targets was present. (*B*) Pre-cc-PAS evaluation consisted of two *gf* assessments (Baseline *gf* 1 and Baseline *gf* 2) interleaved with a LNG task (near transfer) and VS task (far transfer). TMS parameters were based on individual RMT collected at the beginning of each session. (*C*) Different TMS conditions were tested on different days: (i) left IPL TMS pulse either preceding (P → F, ISI = +10 ms), (ii) following (F → P, ISI = −10 ms), or (iii) delivered simultaneously (Simultaneous-TMS, ISI = 0 ms) to the TMS pulse over the MFG. Additionally, a (iv) "Prefrontal-TMS" condition was performed by delivering real TMS over MFG and Sham TMS over IPL, while (v) spontaneous learning was tested by longitudinally assessing cognition without stimulation ("NoStim" condition). (*D*) Post-cc-PAS assessment included two *gf* evaluations (Post TMS *gf* 1, Post TMS *gf* 2), interleaved with an LNG (near transfer) and VS task (far transfer) administrated in reverse order with respect to pre-cc-PAS.

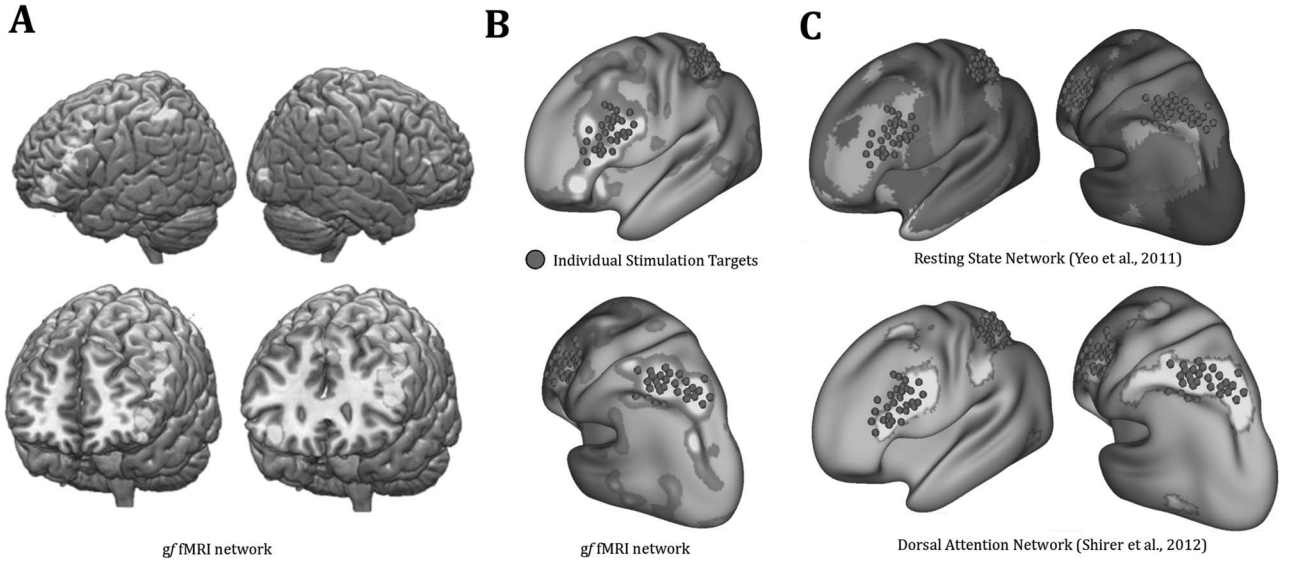

Figure 2. TMS targets based on fMRI data. (*A*) A meta-analytic map of *gf* fMRI activation patterns (Santarnecchi et al. 2017) used to derive individual FC maps. (*B*) Overlap between individual TMS targets of the current study and *gf* network. (*C*) Overlap between TMS targets and known resting state networks parcellations.

the response to cc-PAS, by looking at seed-based functional connectivity (Biswal et al. 2010; Sporns 2014) of TMS targets. We hypothesized that individuals with stronger functional connectivity between the nodes of the *gf* network targeted by TMS will benefit less from cc-PAS, due to the already high level of synchronicity among the stimulated sites.

Materials and Methods

Participants

Thirty healthy individuals (13 females) (mean ± standard deviation (SD), 25.43 years ± 3.69) were recruited through flyers at the University of Siena School of Medicine (Italy). On average, participants carried out a total amount of five visits (Fig. 1). A comprehensive cognitive assessment and MRI acquisition were performed at a baseline assessment visit (Fig. 1A). In each of the following TMS visits, participants solved four parallel versions of a validated *gf* task (Sandia matrices, see dedicated paragraph below), before and after neuronavigated cc-PAS. To evaluate the specificity of cc-PAS effects on *gf* problem solving, as well as to exclude possible effects due to generalized increase in arousal, an inhibition and an attentional task were administered before (Fig. 1B) and after (Fig. 1D) each TMS session.

The experiment consisted of five conditions (Fig. 1C), addressing the impact of cc-PAS with different delays between the first and second TMS pulse (conditions with ISI = +10 ms, i.e., P → F and −10 ms, F → P), as well as three control conditions: (1) a nonassociative TMS condition, with ISI = 0 ms (Simultaneous-TMS); (2) stimulation over one single *gf* region (Prefrontal-TMS) previously reported as associated with cognitive enhancement induced by brain stimulation (Boroojerdi et al. 2001; Santarnecchi et al. 2013); and (3) repeated *gf* assessment following the same experimental design but with no TMS (NoStim), to assess the impact of spontaneous *gf*-related learning induced by repeated cognitive testing in healthy young adults. To avoid learning effects across sessions as well as excessive fatigue due to the length of each cc-PAS session (~3 h), TMS sessions were separated by at least 3 days. The study was approved by the Ethical Committee of the University of Siena. An informed consent was obtained from all participants according to the Declaration of Helsinki. Participants were given 30€ for the entire study.

Baseline Visit

MRI Session

Structural and functional MRI sequences were acquired to derive individualized stimulation targets for TMS a few days prior to the TMS sessions, together with an extensive cognitive evaluation (see next paragraph and Fig. 1A). MRI session lasted approximately 1 h. Details about the MRI sequences (i.e., T1-weighted, T2-FLAIR, and T2-blood oxygen level–dependent [BOLD] resting state fMRI) and image preprocessing are included as part of the Supplementary Materials.

Cognitive Evaluation

A comprehensive cognitive profile was obtained via 10 cognitive tasks measuring flexibility (Global–Local features task abilities) (Navon 1977), switching (Preparing to Overcome Prepotency task) (Rosano et al. 2005), inhibition (LNG) (Thorell et al. 2009), attention (VS) (Treisman and Gelade 1980), verbal (Digit Span) (Wechsler 1981) and visuospatial (Change Localization) (Luck and Vogel 1997) working-memory, *gf* (Raven's Advanced Progressive Matrices [RPM]) (Raven et al. 1998), premorbid intelligence quotient (Test di Intelligenza Breve) (Sartori et al. 1997), and frontal lobe functioning (Cognitive Estimation Task) (Della Sala et al. 2003). The tasks were presented using E-Prime 2.0 Professional (Psychology Software Tools; www.pstnet.com) on a 19-inch screen located 80 cm away from the participants. See Supplementary Material for a detailed description of each task.

Longitudinal *gf* Assessment

The *gf* measures were based on the Sandia matrices (Matzen et al. 2010) (Fig. 1), an abstract reasoning task originally created to mimic the gold standard *gf* test (RPM), while offering the possibility for repeated *gf* assessments via a large set of alternative stimuli (~3000). Each matrix is composed of a 3 × 3 grid, with each cell in the grid containing a set of shapes. A blank cell in position 3–3 of the grid (bottom right) is present. Participants are required to complete the matrix by selecting one of eight alternative solutions. In the present experiment, participants responded by pressing the corresponding key on a PC numerical keyboard (1–8). A maximum response time of 60 s was allowed for each matrix, after which the next matrix appeared. Differently from the original RPM, where the progression of the stimuli is fixed and the stimuli do not reflect a specific reasoning subprocess, the Sandia stimuli were created with a fine characterization of each stimuli features, including the type and number of operations required (e.g., subtraction of color, matching of stimuli dimension, no spatial rotation). This allowed to create balanced, parallel versions of the task that can be used for longitudinal assessment. Moreover, stimuli can be divided into two main categories, reflecting relational and logical reasoning. Relational matrices can be solved by capturing variations in the features of shapes across cells in the grid (i.e., color, size, orientation, number, shape), with some features remaining constant while others vary. Only the highest difficulty trials were used, with variations in three of the five features, referred to as "three-relation" matrices. Conversely, logic matrices required participants to perform logical operations across the matrix (i.e., conjunction, disjunction, or exclusive disjunction, known as AND, OR, and XOR boolean functions, respectively). Each *gf* assessment was composed by 21 trials of Relational and Logical trials (42 matrices total, time limit for each matrix = 60 s), presented in a randomized order. At each visit, participants performed four parallel versions of Sandia matrices (Baseline *gf* 1, Baseline *gf* 2, Post TMS *gf* 1, Post TMS *gf* 2). Before Baseline *gf* 1, participants performed an additional short training to familiarize with the stimuli and reduce novelty effects.

Experimental Visits

Each TMS visit lasted ~3 h. First, participants performed a first set of trials of the Sandia task, which served as a within-session baseline measure (Baseline *gf* 1, Fig. 1B). Then, they performed the near- and far-transfer tasks (see dedicated section below) to evaluate inhibition and attentional levels before cc-PAS. Subsequently, resting motor threshold (RMT) was identified for each participant, targeting the left motor cortex (M1) (see below). RMT was used to define TMS intensity for each participant according to international TMS guidelines (Rossi et al. 2009). Participants were given a short break (~10 min) before being tested with the Sandia task again right before cc-PAS (Baseline *gf* 2), which was then applied continuously for 15 min. During stimulation, subjects were seated on a comfortable reclining chair with both arms relaxed and with their eyes open. Immediately after cc-PAS, participants performed a third version of the Sandia to evaluate acute TMS-induced effects (Post TMS *gf* 1, Fig. 1D). After a 25- to 35-min break (around 1 h after the end of cc-PAS),

the last assessment with Sandia matrices was carried out (Post TMS *gf* 2). Moreover, two additional tasks (VS and LNG) were administrated twice (before and after cc-PAS, in reverse order) to evaluate near- and far-transfer effects. TMS conditions and tasks order were counterbalanced across subjects. Further details on TMS, neuronavigation, targets definition, and cognitive tasks are reported in dedicated sections.

Transfer Measures

Both inhibition (LNG) and selective attention (VS) were evaluated to investigate near and far transfer, respectively (Barnett and Ceci 2002). For more information on the cognitive tasks see the paragraphs below.

Visual Search

VS is considered an index of attentional and perceptual resources, involving the ability to scan the visual field for a particular target among distractors (Treisman and Gelade 1980). The screen is divided into four quadrants filled with an array of randomly placed "T" letters with only one "L" letter. Participants were asked to indicate the quadrant including the "L" as quickly and accurate as possible, by pressing the corresponding key on the laptop keyboard. At the beginning of each trial, a fixation cross was shown at the center of the screen for 2000 ms. The "L" letter randomly occurred 18 times for each quadrant (72 trials total). Participants were given 2 s to respond before the following trial started. Reaction times (RTs) and ACC measures were recorded.

Letter No-Go

The task assessed executive functions, specifically response inhibition. Four parallel version trials were created in order to reduce learning and practice effect. In each version, the "No-Go" stimuli were changed. A stream of random letters was presented at the center of the screen, including the No-Go letter (depending on task version: "X," "K," "W," "Z"). Participants were instructed to press the arrow down key anytime a "Go" letter was presented ("Go" trials; e.g., A…C…F….N…) and to suppress their response when No-Go trials occur ("No-Go" trials). Twenty-five Go letters were randomly used as Go stimuli. Each Go letter was presented 4 times, while the No-Go letter appeared 28 time. Participants completed a total of 128 trials. RTs and ACC were recorded.

fMRI-Guided TMS Targeting

While scalp landmarks based on the 10–20 International EEG system might be suitable for studies aimed at modulating large brain regions (Herwig et al. 2003), modulation of resting state fMRI networks requires further optimization to ensure precise targeting and to account for individual differences in fMRI patterns (Fox et al. 2012). In recent years, few studies have used intrinsic connectivity to identify TMS targets (Hoffman et al. 2007; Eldaief et al. 2011) (for a review, see Fox et al. 2012), promoting the value of individualized stimulation protocols over those based on anatomical landmarks. As shown in Figure 2*A* and *B*, a left-lateralized frontoparietal network based on a task-fMRI meta-analysis map of *gf* activation during matrix-like reasoning tasks (Santarnecchi et al. 2017) (www.tmslab.org/santalab-fluid.php) was identified as target for the present study. Each participant's fMRI data collected during baseline visit was then used to derive individual seed-based functional connectivity maps of the *gf* network. Two targets were identified, approximately corresponding to the left inferior parietal lobule (IPL) and left middle frontal gyrus (MFG), as the most positively correlated nodes in the *gf* network. Two independent investigators (ES, DM) checked both functional connectivity maps and structural MRI data (i.e., T1-weighted images) in order to identify individual hotspots satisfying the following criteria: stimulation sites should (1) be as close as possible to the local maxima of the IPL/MFG clusters; (2) be on the top of a cortical gyrus (avoiding sulci); and (3) represent the shortest perpendicular path connecting the stimulating TMS coil on the scalp and the cortex. High individual variability in TMS targets was evident, with individual nodes showing high heterogeneity across participants (Fig. 2*C*). To stimulate IPL, the coil was positioned with a 15° angle with respect to the midline, inducing a posterior–anterior current direction (Koch et al. 2007). The coil was positioned with a 45° angle for MFG stimulation (Boschin et al. 2017). Once optimal stimulation nodes were identified, target sites were loaded into the neuronavigation software (see dedicated paragraph).

cc-PAS Protocol

cc-PAS intervention consisted of 180 paired TMS pulses over the left hemisphere that were continuously delivered every 5 s (2 Hz) over a total period of 15 min. The conditioning (first TMS pulse) stimulus was set at an intensity of 90% of RMT, while the test stimulus (second TMS pulse) was applied at an intensity of 120% of the ipsilateral RMT.

The experiment consisted of two active cc-PAS conditions (P → F and F → P). Depending on the condition, left IPL stimulation could precede (P → F, ISI = +10 ms) or follow (F → P, ISI = −10 ms) the TMS pulse on MFG. The 10 ms ISI was picked based on intracortical facilitation TMS protocol, which has been shown to induce STDP in the posterior parietal cortex-M1 connection when cc-PAS was delivered within a temporal window of 5–20 ms (Stefan et al. 2000; Koch et al. 2013; Casula et al. 2016). The same 10-ms protocol has been recently used to modulate TMS-EEG activity of a frontoparietal network, showing its efficacy in modulating long-range connections (Casula et al. 2016), as well as in an fMRI study aimed at modulating connectivity between resting state networks (Santarnecchi et al. 2018). Three additional control conditions were included (1) a cc-PAS condition with both pulses on MFG and IPL delivered at the same time (Simultaneous-TMS, ISI = 0 ms), (2) a TMS condition with active stimulation over MFG and sham stimulation over IPL (Prefrontal-TMS hereafter), and (3) a no stimulation (NoStim) condition aimed at evaluating spontaneous learning during repeated *gf* testing. During Prefrontal-TMS, stimulation was performed delivering real TMS over MFG and sham TMS over IPL (achieved by tilting the coil 90°). The NoStim condition was carried out by tilting both TMS coils by 90°.

Electromyography and Resting Motor Threshold Procedures

TMS was applied using a custom-made STM9000 magnetic stimulator (Ates-EBNeuro) connected to two independent 70-mm figure-8 coils. At the beginning of each visit, RMT was determined for the left M1 "hot spot," corresponding to the scalp location where TMS intensity was sufficient to evoke a motor response (~ 50 uV) in the right first dorsal interosseous (FDI) muscle in at least 50% of the trials. Electromyographic

activity was recorded with the active electrode positioned over the belly of the FDI muscle, while the reference electrode was placed over the metacarpophalangeal joint of the index finger. To stimulate left M1, the TMS coil was positioned at an angle of ~45° with respect to the midline. RMT was used as a corticospinal excitability index and used to set individual cc-PAS intensity for both TMS coils at each visit.

Neuronavigation

Two independent neuronavigation softwares (BrainNET, EBneuro Ltd) with infrared cameras (Polaris Vicra, NDI) were used to simultaneously control the two TMS coils. The T1-weighted and fMRI images of each participant were uploaded on the neuronavigation software, and a coregistration procedure was performed using scalp landmarks (nasion, vertex, and the two preauricular points). The coils were calibrated using an in-house algorithm based on five landmarks specific for the device. During cc-PAS, the software provided online auditory and/or visual feedbacks about coil displacement, allowing the investigators to keep the desired coil orientation/rotation/distance during the entire stimulation session.

Behavioral Data Analysis

ACC and RTs were evaluated using the Statistical Package for the Social Sciences (SPSS) software, version 20 (IBM Corp 2011). Data were filtered for outliers (mean ± 2 SD and subjects having ACC > 95% at Baseline *gf* 1). Analysis of RTs was based on RTs for correct trials. Sandia gains (ΔRTs and ΔACC) were computed by subtracting the poststimulation average (mean of Post TMS *gf* 1 and Post TMS *gf* 2) with respect to performance at Baseline *gf* 2, in order to compare longitudinal changes in *gf* "across participants." The critical *P* value was adjusted using Bonferroni correction for multiple comparisons. We conducted a repeated measure analysis of variance comparing the behavioral performance after the five different TMS conditions (within-subject factor "STIMULATION"; 5 levels: P → F, F → P, Simultaneous-TMS, Prefrontal-TMS, and NoStim) and different reasoning processes (within-subject factor "REASONING"; two levels: logical and relational). Mean standard error and *P* values for each contrast are summarized in Supplementary Table 1.

Connectivity-Based Predictors of Response to cc-PAS Stimulation

Given the identification of the TMS targets based on the functional connectivity data, we hypothesized that baseline individual fMRI patterns might predict the response to network stimulation. A multiple regression analysis was implemented using CONN-fMRI functional connectivity toolbox v17f (Whitfield-Gabrieli and Nieto-Castanon 2012), looking at the predictive power of seed-based connectivity maps based on the *gf* network over individual changes in performance after cc-PAS, calculated both for logical and relational reasoning. The *gf* gains in performance (ΔACC) were entered as second-level covariates of interest for those TMS conditions showing a significant modulation after cc-PAS (logical reasoning P → F and relational reasoning F → P). The model resulted in voxel-wise maps showing regions whose positive or negative connectivity with the *gf* network at baseline predicted the response to cc-PAS. Statistical thresholds were as follows: *P* value < 0.001 with false discovery correction (at voxel level) and *P* value < 0.001 uncorrected (at cluster level). Analyses were performed in MNI space. The results of the multiple regression analysis are reported as Supplementary Materials (see Supplementary Fig. 1).

Behavioral Predictors of Response to cc-PAS

Specific links between baseline cognitive profile variables and *gf* gains after cc-PAS were further tested. Specifically, we conducted two separated multiple regression analysis ("The Goodness of Fit of Regression Formulae and the Distribution of Regression Coefficients" 1926) entering *gf* gains (i.e., increase in ACC) after F → P and P → F cc-PAS as dependent variables, while cognitive tasks where considered independent variables.

Activation Likelihood Estimation Meta-Analysis Maps

To interpret the results of the cognitive transfer analysis, ad hoc meta-analytic fMRI maps for the LNG and VS tasks were created. We conducted a literature search through PubMed and Google Scholar to identify neuroimaging studies implementing LNG or VS (for the list of included studies, see Supplementary Table 2). We analyzed the activation coordinates using a random-effects meta-analysis implemented using GingerALE 2.3.6 software (UT Health Science Center Research Imaging Institute) (Laird et al. 2005; Eickhoff et al. 2009, 2012; Turkeltaub et al. 2012). The resulting maps were used for a quantitative overlap analysis (using DICE overlap coefficient) (Dice 1945) between inhibition/attention task-fMRI patterns and the *gf* network, possibly explaining the likelihood of transfer across functions. For additional details on the activation likelihood estimation method, inclusion/exclusion criteria, and results of the analysis, please see Supplementary Information (Supplementary Tables 2 and 4).

RESULTS

Behavioral Changes

Accuracy

A significant interaction REASONING × STIMULATION was found ($F_{(1,28)} = 6.11$, $P < 0.0001$). Moreover, a significant main effect of STIMULATION was found ($F_{(1,28)} = 3.84$, $P = 0.006$), while no significant main effect of REASONING was found ($F_{(1,28)} = 0.13$, $P = 0.71$).

As for logical reasoning (Fig. 3A), stimulation of the frontoparietal network following a posterior to anterior gradient was hypothesized to be more effective. As expected, behavioral responses after P → F stimulation were significantly more accurate compared to Simultaneous-TMS (mean difference = 8%, $P = 0.002$), F → P stimulation (mean difference = 13%, $P < 0.0001$), Prefrontal-TMS (mean difference = 9%, $P < 0.0001$), and NoStim (mean difference = 6%, $P = 0.05$). Participants were less accurate during F → P condition with respect to Simultaneous-TMS (mean difference = −4%, $P = 0.04$), Prefrontal-TMS (mean difference = −4%, $P = 0.01$), and NoStim (mean difference = −7%, $P = 0.02$).

As for relational reasoning (Fig. 3B), frontoparietal network stimulation with anterior to posterior associative direction was supposed to enhance individual *gf* performance. According to the hypothesis, pairwise comparison revealed a significantly higher ACC for F → P stimulation with respect to Simultaneous-TMS (mean difference = 6%, $P = 0.01$), Prefrontal-TMS (mean difference = 4%, $P = 0.006$), and NoStim (mean difference = 6%, $P = 0.002$) conditions.

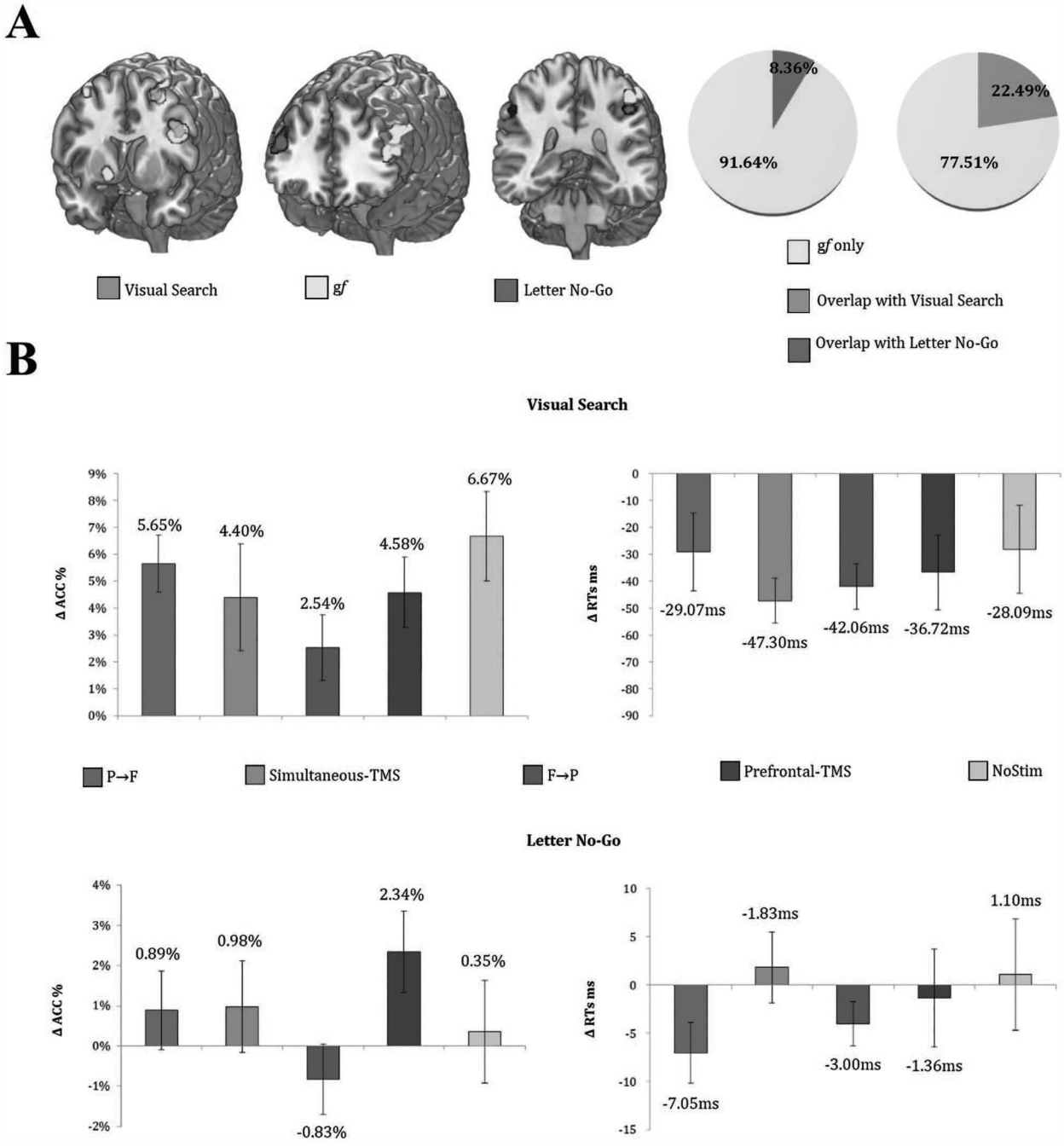

Figure 3. Effects on *gf* performance. Significant changes in logical reasoning performance (i.e., pre- and post-delta ACC) were observed after P → F cc-PAS (*A*), whereas a significant enhancement in relational reasoning was found after F → P cc-PAS (*B*). All ACC values were normalized to baseline. Error bars represent ±1 standard error of the mean (SEM). For cc-PAS effects on RTs, please refer to the Supplementary Materials. Note: * = $P < 0.05$; ** = $P < 0.01$; *** = $P < 0.001$.

Response Times

A significant interaction REASONING × STIMULATION was found ($F_{(1,28)} = 6.78$, $P < 0.0001$). Moreover, a significant main effect of STIMULATION was reported ($F_{(1,28)} = 3.43$, $P = 0.007$), while no significant effect of REASONING was found ($F_{(1,28)} = 0.78$, $P = 0.83$).

Pairwise post hoc comparisons for logical reasoning revealed that, after receiving P → F cc-PAS, participants were significantly faster as compared to F → P (mean difference = −943 ms, $P = 0.02$), Simultaneous-TMS (mean difference = −904 ms, $P = 0.001$), and Prefrontal-TMS (mean difference = −790, $P < 0.0001$). Moreover, RTs in the NoStim condition were faster than P → F (mean difference = −1181 ms, $P = 0.02$), Simultaneous-TMS (mean difference = −1142 ms, $P = 0.002$), and Prefrontal-TMS (mean difference = −1029 ms, $P = 0.001$).

Post hoc comparisons for relational reasoning showed faster responses for F → P as compared to Simultaneous-TMS (mean difference = −1044 ms, $P < 0.0001$) and Prefrontal-TMS (mean difference = −799 ms, $P < 0.0001$). Additionally, after NoStim, participants were faster as compared to Simultaneous-TMS (mean

difference = −1160 ms, $P = 0.002$) and Prefrontal-TMS (mean difference = −915 ms, $P = 0.003$). For further details, see Supplementary Table 1.

Transfer Effects

Quantitative spatial overlap analysis (DICE coefficient) (Dice 1945) revealed little overlap between LNG/VS activation patterns and the *gf* network. As shown in Figure 4, LNG displays a right-lateralized BOLD activation pattern (Garavan et al. 1999), with greater activity over the right MFG and IPL. A cluster in the left hemisphere was also present, marginally overlapping (8.36%) with a *gf*-associated region. As for VS, a prevalent activation in the left inferior frontal gyrus, left MFG, and right superior parietal lobule was found. A slightly higher overlap with the *gf* network was present (22.49%) as compared to LNG, especially in the left MFG.

Accordingly to the low degree of overlap between LNG/VS fMRI activation patterns and TMS targets/*gf* network, no significant main effects of STIMULATION were found for both ACC ($F_{(4,112)} = 2.08$, $P = 0.08$) and RTs ($F_{(4,112)} = 1.44$, $P = 0.22$) of LNG. As for VS, no significant main effect of STIMULATION was reported for ACC ($F_{(4,112)} = 1.70$, $P = 0.15$) and RTs ($F_{(4,112)} = 1.19$, $P = 0.31$). For further details, see Supplementary Table 3.

Behavioral Predictors of Response to cc-PAS

We also looked at the predictive power of individual differences in age, gender, and baseline cognitive performance over the response to cc-PAS (for details on the cognitive tasks, see the Materials and Methods section). Overall, no significant predictors were identified. Further details regarding the behavioral multiple regression analysis results are provided in the Supplementary Materials.

Discussion

Previous studies have shown how cc-PAS might induce STDP between interconnected regions, modulating their spontaneous connectivity and corresponding behavior in the motor and visual systems (Koch et al. 2013; Romei et al. 2016), with few evidences in high-order cognitive domain (Kohl et al. 2018; Nord et al. 2019). Current results showed how a relatively brief cc-PAS protocol over associative cortical regions might be able to increase cognitive abilities such as logical and relational reasoning in humans.

Increase of *gf* performance were evident for both experimental conditions (P → F and F → P). The observed effects with ISI = 10 ms compared to the other stimulation conditions (i.e., Simultaneous-TMS, Prefrontal-TMS) well match previous studies demonstrating STDP effects within a time window between 5 and 20 ms for both interhemispheric (Rizzo et al. 2009) and intrahemispheric connections (Koch et al. 2013) in humans. Specifically, 10 ms ISI has been associated with induction of changes in the spectral coherence between the left posterior parietal cortex and ipsilateral M1 (Veniero et al. 2013), while a recent TMS-EEG study has demonstrated changes in the spectral oscillatory power of the dorsolateral PFC following cc-PAS over two frontoparietal sites similar to those adopted in the present study (Casula et al. 2016).

By tailoring the TMS intervention on individual functional connectivity patterns, current results represent the first evidence of a transient behavioral change in *gf* following a TMS cc-PAS protocol. Moreover, the boosting effect is dependent by the direction of stimulation (and presumably of the induced associative plasticity), with a better performance after P → F for logical trials and after F → P for relational trials. Results are somewhat consistent with previous notions that logical reasoning requires more prefrontal engagement, while relational processing mostly load on parietal structures (Prado et al. 2010). Both feedforward and feedback flow of cognitive processing during intelligence-related problem solving have been proposed within the widely accepted parietofrontal integration theory of intelligence (Jung and Haier 2007), suggesting cc-PAS as an effective tool to causally validate cognitive models in humans.

Remarkably, a decrease in *gf* performance was reported specifically for logical reasoning when stimulation was applied following an anterior to posterior direction (F → P). The observed effects match previous evidences demonstrating a posterior to anterior processing flow flow during abstract reasoning tasks (Li et al. 2015; Siegel et al. 2015). Since logical reasoning seems to load mostly on prefrontal brain structures (Prado et al. 2010), reinforcing interregional brain dynamics in the opposite direction might have been detrimental.

Apart from network effects involving associative plasticity between stimulated regions, our results could also reflect the modulation of local activity in one of the two targets. This hypothesis would fit with previous cc-PAS evidence in the motor (Koch et al. 2013) and visual systems (Romei et al. 2016) reporting a modulation of neurophysiological responses (i.e., EEG spectral power), mostly involving the receiving end of the two stimulated regions (i.e. A → B, effect on B; B → A, effect on A) (Casula et al. 2016). According to this model, P → F stimulation would mainly benefit local processing of prefrontal sites, while F → P would affect parietal lobe function. Interestingly, and as observed in our data, P → F cc-PAS over IPL → MFG would translate into enhancement of MFG activity, which has been linked to logical reasoning both in neuroimaging (Prado et al. 2010) and brain stimulation studies (Santarnecchi et al. 2013; Pahor and Jaušovec 2014; Neubauer et al. 2017). Conversely, F → P (MFG → IPL) would show effects on IPL/relational reasoning process. However, in the present study, stimulation of prefrontal sites alone (i.e., slow frequency TMS, one pair of pulses every 4–5 seconds, ∼0.2 Hz) did not elicit modulation of logical reasoning, therefore suggesting the associative nature of cc-PAS being the key principle behind the observed cognitive effects. Moreover, a recent study has tested the impact of cc-PAS over two cortical sites while looking at changes in functional connectivity using fMRI, reporting no local effects in face of a specific modulation of the connectivity between stimulated network nodes (Santarnecchi et al. 2018), supporting the associative nature of cc-PAS effects.

As for cognitive transfer, stimulation over *gf*-related regions did not induce any transfer of cognitive abilities in our sample. We originally hypothesized that abilities related to *gf*, such as inhibition and attention (Woolgar et al. 2010), would also benefit from cc-PAS. However, no significant modulation of performance was found, except for a generalized decrease in RTs after cc-PAS (but not after Prefrontal-TMS), likely due to greater arousal generated by the TMS setup and dual-site stimulation. We also performed an original meta-analysis of fMRI activations specific for the two transfer tasks adopted in the study (i.e., LNG, VS), looking at the overlap between stimulated brain regions and fMRI activations typically reported for "transfer" cognitive functions. TMS stimulation sites and fMRI activation maps showed relatively little spatial overlap, suggesting this as

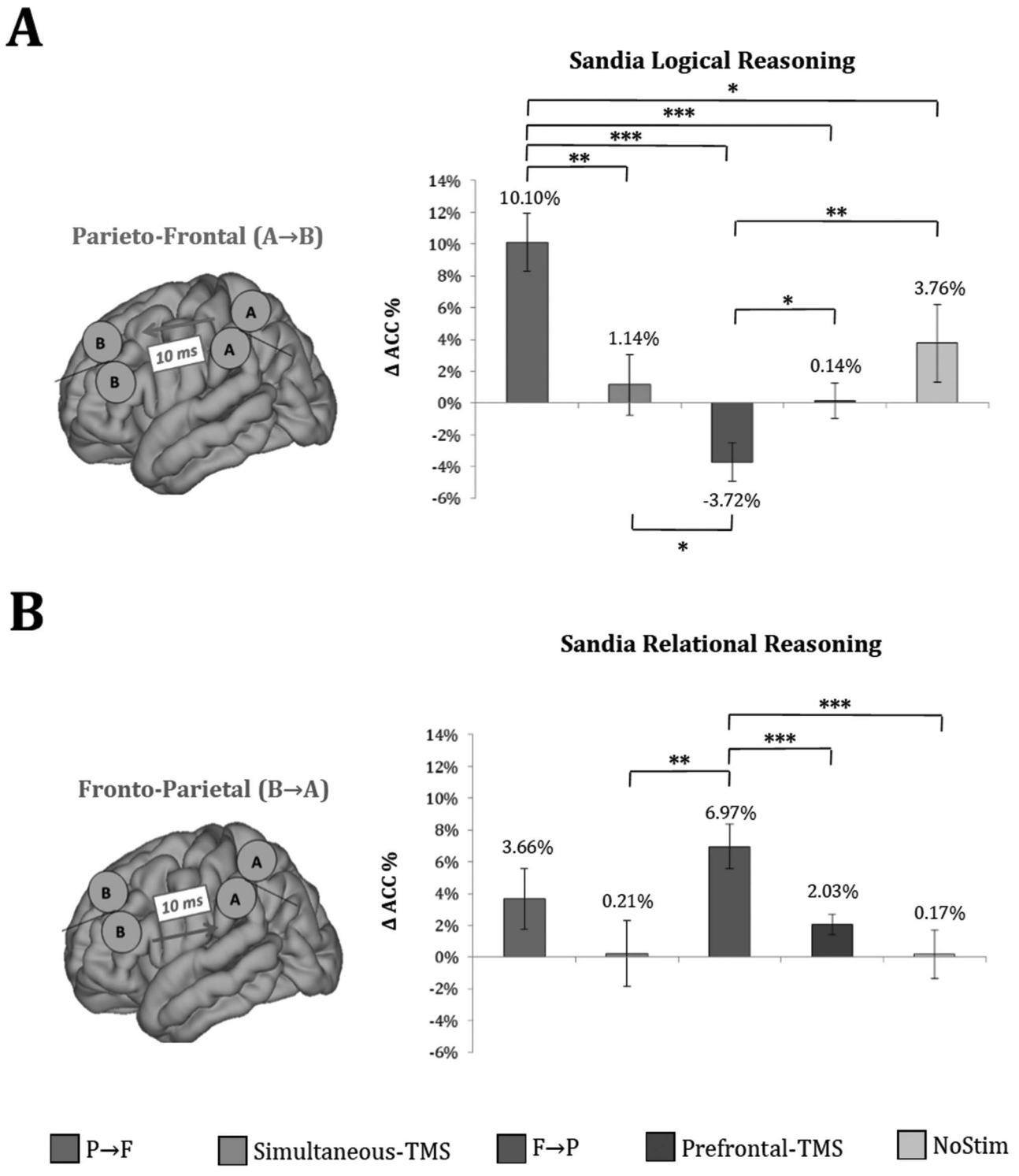

Figure 4. Near and far transfer. (*A*) Average patterns of fMRI activation during the transfer tasks (VA, LNG) and *gf* tasks, as well as their quantitative overlap (*B*). No significant changes in ACC and RTs were observed for the transfer tasks after any TMS condition. Error bars represent ±1 SEM.

a potential reason for the lack of transfer. Future studies should select cognitive tasks with different degrees of overlap with the cognitive function targeted by cc-PAS, systematically testing the possibility of inducing transfer when targeting common connectivity pathways.

Limitations of the Study

The relatively small sample requires additional work to confirm the present results. Moreover, even though the study suggests the feasibility of modulating specific interregional brain dynamics in a timing-dependent manner, the observed changes in *gf*

scores possibly reflect (among other interpretations) problem-solving strategy refinement (Hayes et al. 2015), nonspecific effects of TMS (Luber and Lisanby 2014), changes in functional connectivity or cerebral blood flow (Strafella and Paus 2001). The understanding of the neurophysiological substrates of cc-PAS effects requires more in-depth investigations based on, for example, TMS-EEG (Komssi and Kähkönen 2006), arterial spin labeling (Alsop et al. 2015), positron emission tomography (Bailey et al. 2005), and diffusion tensor imaging (DTI) (Basser et al. 2000). Follow-up studies should also investigate the potential cumulative impact of repeated cc-PAS sessions.

As for the specificity of the 10 ms ISI, we cannot exclude that slightly longer (e.g., 20 ms) or shorter (e.g., 5 ms) ISIs could induce similar STDP effects within the *gf* network (or even amplify it), as observed for the motor system (Weise et al. 2006). Indeed, it could be speculated that the relatively large distance between the two nodes (i.e., MFG and IPL) might lead to a gradual shift of the proper timing required to induce long-term potentiation or long-term depression compared to the conventional Hebbian rule (Froemke et al. 2010). Further experiments guided by a quantification of ISI based on brain oscillations (by means of combined TMS-EEG approaches) or white matter connectivity (via DTI) should be considered in order to estimate proper conduction times within the network of interest.

Conclusion

Current results reveal the feasibility of modulating specific interregional brain dynamics in a timing and direction-dependent manner, within the Hebbian plasticity framework. If validated and optimized, cc-PAS might translate into a valuable tool for cognitive enhancement in healthy subjects, as well as a therapeutic tool for neurological and psychiatric populations with known specific connectivity alterations linked to cognitive deficits.

Supplementary Material

Supplementary material is available at *Cerebral Cortex* online.

Funding

Office of the Director of National Intelligence; Intelligence Advanced Research Projects Activity (grant 2014-13121700007 to P.-L.A. and S.E). Berenson-Allen Foundation; Sidney R. Baer Jr Foundation (grants from the National Institutes of Health, R01HD069776, R01NS073601, R21 MH099196, R21 NS082870, R21 NS085491, R21 HD07616 to P.-L.A.); Harvard Catalyst|The Harvard Clinical and Translational Science Center (NCRR and the NCATS National Institutes of Health, UL1 RR025758 to P.-L.A.). Beth Israel Deaconess Medical Center via the Chief Academic Officer Award 2017; the Defense Advanced Research Projects Agency (HR001117S0030 to S.E.); Cognito Therapeutics.

Notes

The authors would like to thank all participants who took part in the study and for their efforts. The content of this paper is solely the responsibility of the authors and does not necessarily represent the official policies or endorsements, either expressed or implied, of the Office of the Director of National Intelligence, Intelligence Advanced Research Projects Activity, or the US Government, of Harvard Catalyst, Harvard University and its affiliated academic health care centers, the National Institutes of Health, or the Sidney R. Baer Jr Foundation. *Conflict of interest*: All authors report no conflict of interest.

References

Alsop DC, Detre JA, Golay X, Günther M, Hendrikse J, Hernandez-Garcia L, Lu H, MacIntosh BJ, Parkes LM, Smits M et al. 2015. Recommended implementation of arterial spin-labeled perfusion MRI for clinical applications: a consensus of the ISMRM perfusion study group and the European consortium for ASL in dementia. *Magn Reson Med*. 73:102–116.

Au J, Buschkuehl M, Duncan GJ, Jaeggi SM. 2016. There is no convincing evidence that working memory training is NOT effective: a reply to Melby-Lervåg and Hulme (2015). *Psychon Bull Rev*. 23:331–337.

Bailey DL, Townsend DW, Valk PE, Maisey MN, editors. 2005. *In: Positron emission tomography: basic sciences*. London: Springer-Verlag.

Barnett SM, Ceci SJ. 2002. When and where do we apply what we learn? A taxonomy for far transfer. *Psychol Bull*. 128:612–637.

Basser PJ, Pajevic S, Pierpaoli C, Duda J, Aldroubi A. 2000. In vivo fiber tractography using DT-MRI data. *Magn Reson Med*. 44:625–632.

Beard JL, Hendricks MK, Perez EM, Murray-Kolb LE, Berg A, Vernon-Feagans L, Irlam J, Isaacs W, Sive A, Tomlinson M. 2005. Maternal iron deficiency anemia affects postpartum emotions and cognition. *J Nutr*. 135:267–272.

Biswal BB, Mennes M, Zuo XN, Gohel S, Kelly C, Smith SM, Beckmann CF, Adelstein JS, Buckner RL, Colcombe S et al. 2010. Toward discovery science of human brain function. *Proc Natl Acad Sci USA*. 107:4734–4739.

Boroojerdi B, Phipps M, Kopylev L, Wharton CM, Cohen LG, Grafman J. 2001. Enhancing analogic reasoning with rTMS over the left prefrontal cortex. *Neurology*. 56:526–528.

Boschin EA, Mars RB, Buckley MJ. 2017. Transcranial magnetic stimulation to dorsolateral prefrontal cortex affects conflict-induced behavioural adaptation in a Wisconsin card sorting test analogue. *Neuropsychologia*. 94:36–43.

Casula EP, Pellicciari MC, Picazio S, Caltagirone C, Koch G. 2016. Spike-timing-dependent plasticity in the human dorsolateral prefrontal cortex. *Neuroimage*. 143:204–213.

Cattell RB. 1963. Theory of fluid and crystallized intelligence: a critical experiment. *J Educ Psychol*. 54:1–22.

Deary IJ, Strand S, Smith P, Fernandes C. 2007. Intelligence and educational achievement. *Intelligence*. 35:13–21.

Della Sala S, MacPherson SE, Phillips LH, Sacco L, Spinnler H. 2003. How many camels are there in Italy? Cognitive estimates standardised on the Italian population. *Neurol Sci Off J Ital Neurol Soc Ital Soc Clin Neurophysiol*. 24:10–15.

Dice LR. 1945. Measures of the amount of ecologic association between species. *Ecology*. 26:297–302.

Eickhoff SB, Bzdok D, Laird AR, Kurth F, Fox PT. 2012. Activation likelihood estimation meta-analysis revisited. *NeuroImage*. 59:2349–2361.

Eickhoff SB, Laird AR, Grefkes C, Wang LE, Zilles K, Fox PT. 2009. Coordinate-based activation likelihood estimation meta-analysis of neuroimaging data: a random-effects approach based on empirical estimates of spatial uncertainty. *Hum Brain Mapp*. 30:2907–2926.

Eldaief MC, Halko MA, Buckner RL, Pascual-Leone A. 2011. Transcranial magnetic stimulation modulates the brain's intrinsic activity in a frequency-dependent manner. *Proc Natl Acad Sci USA*. 108:21229–21234.

Filicková M, Ropovik I, Bobaková M, Kovalcíková I. 2015. The relationship between fluid intelligence and learning potential: is there an interaction with Attentional control? *J Pedagogy*. 6:25–41.

Fisher RA. 1922. The Goodness of Fit of Regression Formulae, and the Distribution of Regression Coefficients. *Journal of the Royal Statistical Society*. 85:597–612.

Fox MD, Halko MA, Eldaief MC, Pascual-Leone A. 2012. Measuring and manipulating brain connectivity with resting state functional connectivity magnetic resonance imaging (fcMRI) and transcranial magnetic stimulation (TMS). *NeuroImage*. 62:2232–2243.

Froemke RC, Letzkus JJ, Kampa BM, Hang GB, Stuart GJ. 2010. Dendritic synapse location and neocortical spike-timing-dependent plasticity. *Front Synaptic Neurosci*. 2.

Garavan H, Ross TJ, Stein EA. 1999. Right hemispheric dominance of inhibitory control: an event-related functional MRI study. *Proc Natl Acad Sci USA*. 96:8301–8306.

Gard T, Taquet M, Dixit R, Hölzel BK, de Montjoye Y-A, Brach N, Salat DH, Dickerson BC, Gray JR, Lazar SW. 2014. Fluid intelligence and brain functional organization in aging yoga and meditation practitioners. *Front Aging Neurosci*. 6.

Gottfredson LS. 2002. Where and Why g Matters:Not a Mystery. Hum Perform. 15:25–46.

Gottfredson LS, Deary IJ. 2004. Intelligence predicts health and longevity, but why? *Curr Dir Psychol Sci*. 13:1–4.

Gow D, Rothwell J, Hobson A, Thompson D, Hamdy S. 2004. Induction of long-term plasticity in human swallowing motor cortex following repetitive cortical stimulation. *Clin Neurophysiol Off J Int Fed Clin Neurophysiol*. 115:1044–1051.

Guse B, Falkai P, Gruber O, Whalley H, Gibson L, Hasan A, Obst K, Dechent P, McIntosh A, Suchan B et al. 2013. The effect of long-term high frequency repetitive transcranial magnetic stimulation on working memory in schizophrenia and healthy controls—a randomized placebo-controlled, double-blind fMRI study. *Behav Brain Res*. 237:300–307.

Haier RJ. 2014. Increased intelligence is a myth (so far). *Front Syst Neurosci*. 8:34.

Hayes TR, Petrov AA, Sederberg PB. 2015. Do we really become smarter when our fluid-intelligence test scores improve? *Intelligence*. 48:1–14.

Herwig U, Satrapi P, Schönfeldt-Lecuona C. 2003. Using the international 10–20 EEG system for positioning of transcranial magnetic stimulation. *Brain Topogr*. 16:95–99.

Hoffman RE, Hampson M, Wu K, Anderson AW, Gore JC, Buchanan RJ, Constable RT, Hawkins KA, Sahay N, Krystal JH. 2007. Probing the pathophysiology of auditory/verbal hallucinations by combining functional magnetic resonance imaging and transcranial magnetic stimulation. *Cereb Cortex*. 17:2733–2743.

Horn JL, Cattell RB. 1966. Refinement and test of the theory of fluid and crystallized general intelligences. *J Educ Psychol*. 57:253–270.

Houdé O, Zago L, Mellet E, Moutier S, Pineau A, Mazoyer B, Tzourio-Mazoyer N. 2000. Shifting from the perceptual brain to the logical brain: the neural impact of cognitive inhibition training. *J Cogn Neurosci*. 12:721–728.

Corp IBM. 2011. *BM SPSS Statistics for Windows, Version 20.0*. Armonk, NY: IBM Corp.

Jung RE, Haier RJ. 2007. The parieto-frontal integration theory (P-FIT) of intelligence: converging neuroimaging evidence. *Behav Brain Sci*. 30:135–154 discussion 154-187.

Koch G, Fernandez Del Olmo M, Cheeran B, Ruge D, Schippling S, Caltagirone C, Rothwell JC. 2007. Focal stimulation of the posterior parietal cortex increases the excitability of the ipsilateral motor cortex. *J Neurosci Off J Soc Neurosci*. 27:6815–6822.

Koch G, Ponzo V, Di LF, Caltagirone C, Veniero D. 2013. Hebbian and anti-Hebbian spike-timing-dependent plasticity of human cortico-cortical connections. *J Neurosci Off J Soc Neurosci*. 33:9725–9733.

Kohl S, Hannah R, Rocchi L, Nord CL, Rothwell J, Voon V. 2019. Cortical paired associative stimulation influences response inhibition: cortico-cortical and cortico-subcortical networks. *Biol Psychiatry*. 85:355–363.

Komssi S, Kähkönen S. 2006. The novelty value of the combined use of electroencephalography and transcranial magnetic stimulation for neuroscience research. *Brain Res Rev*. 52:183–192.

Laird AR, Fox PM, Price CJ, Glahn DC, Uecker AM, Lancaster JL, Turkeltaub PE, Kochunov P, Fox PT. 2005. ALE meta-analysis: controlling the false discovery rate and performing statistical contrasts. *Hum Brain Mapp*. 25:155–164.

Li F, Tian Y, Zhang Y, Qiu K, Tian C, Jing W, Liu T, Xia Y, Guo D, Yao D et al. 2015. The enhanced information flow from visual cortex to frontal area facilitates SSVEP response: evidence from model-driven and data-driven causality analysis. *Sci Rep*. 5:14765.

Luber B, Lisanby SH. 2014. Enhancement of human cognitive performance using transcranial magnetic stimulation (TMS). *NeuroImage*. 85:961–970.

Luck SJ, Vogel EK. 1997. The capacity of visual working memory for features and conjunctions. *Nature*. 390:279–281.

Matzen LE, Benz ZO, Dixon KR, Posey J, Kroger JK, Speed AE. 2010. Recreating Raven's: software for systematically generating large numbers of Raven-like matrix problems with normed properties. *Behav Res Methods*. 42:525–541.

Müller MB, Toschi N, Kresse AE, Post A, Keck ME. 2000. Long-term repetitive Transcranial magnetic stimulation increases the expression of brain-derived neurotrophic factor and cholecystokinin mRNA, but not neuropeptide tyrosine mRNA in specific areas of rat brain. *Neuropsychopharmacology*. 23:205.

Navon D. 1977. Forest before trees: the precedence of global features in visual perception. *Cognit Psychol*. 9:353–383.

Neisser U, Boodoo G, Jr. Bouchard TJ, Wade A, Brody N, Ceci SJ, Halpern DF, Loehlin JC, Perloff R, Sternberg RJ et al. 1996. Intelligence: knowns and unknowns. *Am Psychol*. 51:77–101.

Neubauer AC, Wammerl M, Benedek M, Jauk E, Jaušovec N. 2017. The influence of transcranial alternating current stimulation (tACS) on fluid intelligence: an fMRI study. *Personal Individ Differ, Robert Stelmack: Differential Psychophysiology*. 118:50–55.

Nord CL, Popa T, Smith E, Hannah R, Doñamayor N, Weidacker K, Bays PM, Rothwell J, Voon V. 2019. The effect of frontoparietal paired associative stimulation on decision-making and working memory. *Cortex J Devoted Study Nerv Syst Behav*. 117:266–276.

Pahor A, Jaušovec N. 2014. The effects of theta transcranial alternating current stimulation (tACS) on fluid intelligence. *Int J Psychophysiol*. 93:322–331.

Prado J, Der Henst J-BV, Noveck IA. 2010. Recomposing a fragmented literature: how conditional and relational arguments engage different neural systems for deductive reasoning. *NeuroImage*. 51:1213–1221.

Raven J, Raven JC, Court JH. 1998. Manual for Raven's Progressive Matrices and Vocabulary Scales. http://www.sjdm.org/dmidi/Raven's_Standard_Progressive_Matrices.html

Reed JA, Einstein G, Hahn E, Hooker SP, Gross VP, Kravitz J. 2010. Examining the impact of integrating physical activity on fluid intelligence and academic performance in an elementary school setting: a preliminary investigation. *J Phys Act Health*. 7:343–351.

Ren X, Schweizer K, Wang T, Xu F. 2015. The prediction of students' academic performance with fluid intelligence in giving special consideration to the contribution of learning. *Adv Cogn Psychol*. 11:97–105.

Rizzo V, Siebner HS, Morgante F, Mastroeni C, Girlanda P, Quartarone A. 2009. Paired associative stimulation of left and right human motor cortex shapes interhemispheric motor inhibition based on a Hebbian mechanism. *CerebCortex*. 19: 907–915.

Rohde TE, Thompson LA. 2007. Predicting academic achievement with cognitive ability. *Intelligence*. 35:83–92.

Romei V, Chiappini E, Hibbard PB, Avenanti A. 2016. Empowering Reentrant projections from V5 to V1 boosts sensitivity to motion. *Curr Biol*. 26:2155–2160.

Rosano C, Aizenstein H, Cochran J, Saxton J, De Kosky S, Newman AB, Kuller LH, Lopez OL, Carter CS. 2005. Functional neuroimaging indicators of successful executive control in the oldest old. *NeuroImage*. 28:881–889.

Rossi S, Hallett M, Rossini PM, Pascual-Leone A. 2009. Safety, ethical considerations, and application guidelines for the use of transcranial magnetic stimulation in clinical practice and research. *Clin Neurophysiol*. 120:2008–2039.

Rossini PM, Rossi S. 2007. Transcranial magnetic stimulation diagnostic, therapeutic, and research potential. *Neurology*. 68:484–488.

Santarnecchi E, Emmendorfer A, Pascual-Leone A. 2017. Dissecting the parieto-frontal correlates of fluid intelligence: a comprehensive ALE meta-analysis study. *Intelligence*. 63: 9–28.

Santarnecchi E, Momi D, Sprugnoli G, Neri F, Pascual-Leone A, Rossi A, Rossi S. 2018. Modulation of network-to-network connectivity via spike-timing-dependent noninvasive brain stimulation. *Hum Brain Mapp*. 39:4870–4883.

Santarnecchi E, Muller T, Rossi S, Sarkar A, Polizzotto NR, Rossi A, Cohen KR. 2016. Individual differences and specificity of prefrontal gamma frequency-tACS on fluid intelligence capabilities. *Cortex J Devoted Study Nerv Syst Behav*. 75:33–43.

Santarnecchi E, Polizzotto NR, Godone M, Giovannelli F, Feurra M, Matzen L, Rossi A, Rossi S. 2013. Frequency-dependent enhancement of fluid intelligence induced by transcranial oscillatory potentials. *Curr Biol*. 23:1449–1453.

Santarnecchi E, Rossi S, Rossi A. 2015. The smarter, the stronger: intelligence level correlates with brain resilience to systematic insults. *Cortex J Devoted Study Nerv Syst Behav*. 64:293–309.

Sartori G, Colombo L, Vallar G, Rusconi ML, Pinarello A. 1997. Test di Intelligenza Breve (T.I.B.). Neuropsy. src/test/tib/index.xml

Schellenberg EG. 2004. Music lessons enhance IQ. *Psychol Sci*. 15:511–514.

Siegel M, Buschman TJ, Miller EK. 2015. Cortical information flow during flexible sensorimotor decisions. *Science*. 348:1352–1355.

Smith SP, Stibric M, Smithson D. 2013. Exploring the effectiveness of commercial and custom-built games for cognitive training. *Comput Hum Behav*. 29:2388–2393.

Sporns O. 2014. Contributions and challenges for network models in cognitive neuroscience. NatNeurosci.

Staufenbiel SM, Brouwer A-M, Keizer AW, van Wouwe NC. 2014. Effect of beta and gamma neurofeedback on memory and intelligence in the elderly. *Biol Psychol*. 95:74–85.

Stefan K, Kunesch E, Benecke R, Cohen LG, Classen J. 2002. Mechanisms of enhancement of human motor cortex excitability induced by interventional paired associative stimulation. *J Physiol*. 543:699–708.

Stefan K, Kunesch E, Cohen LG, Benecke R, Classen J. 2000. Induction of plasticity in the human motor cortex by paired associative stimulation. *Brain*. 123(Pt 3):572–584.

Stern Y. 2002. What is cognitive reserve? Theory and research application of the reserve concept. *JIntNeuropsycholSoc*. 8:448–460.

Stough C, Camfield D, Kure C, Tarasuik J, Downey L, Lloyd J, Zangara A, Scholey A, Reynolds J. 2011. Improving general intelligence with a nutrient-based pharmacological intervention. *Intelligence*. 39:100–107.

Strafella AP, Paus T. 2001. Cerebral blood-flow changes induced by paired-pulse transcranial magnetic stimulation of the primary motor cortex. *J Neurophysiol*. 85:2624–2629.

te Nijenhuis J, van Vianen AEM, van der Flier H. 2007. Score gains on g-loaded tests: No g. *Intelligence*. 35:283–300.

Thorell LB, Lindqvist S, Bergman Nutley S, Bohlin G, Klingberg T. 2009. Training and transfer effects of executive functions in preschool children. *Dev Sci*. 12:106–113.

Treisman AM, Gelade G. 1980. A feature-integration theory of attention. *Cognit Psychol*. 12:97–136.

Turkeltaub PE, Eickhoff SB, Laird AR, Fox M, Wiener M, Fox P. 2012. Minimizing within-experiment and within-group effects in activation likelihood estimation meta-analyses. *Hum Brain Mapp*. 33:1–13.

Veniero D, Ponzo V, Koch G. 2013. Paired associative stimulation enforces the communication between interconnected areas. *J Neurosci*. 33:13773–13783.

Watkins MW, Lei P-W, Canivez GL. 2007. Psychometric intelligence and achievement: a cross-lagged panel analysis. *Intelligence*. 35:59–68.

Wechsler D. 1981. *Wechsler adult intelligence scale—revised*. New York: The Psychological Corporation.

Weise D, Schramm A, Stefan K, Wolters A, Reiners K, Naumann M, Classen J. 2006. The two sides of associative plasticity in writer's cramp. *Brain J Neurol*. 129:2709–2721.

Whitfield-Gabrieli S, Nieto-Castanon A. 2012. Conn: a functional connectivity toolbox for correlated and anticorrelated brain networks. *Brain Connect*. 2:125–141.

Wolters A, Sandbrink F, Schlottmann A, Kunesch E, Stefan K, Cohen LG, Benecke R, Classen J. 2003. A temporally asymmetric Hebbian rule governing plasticity in the human motor cortex. *J Neurophysiol*. 89:2339–2345.

Woolgar A, Parr A, Cusack R, Thompson R, Nimmo-Smith I, Torralva T, Roca M, Antoun N, Manes F, Duncan J. 2010. Fluid intelligence loss linked to restricted regions of damage within frontal and parietal cortex. *Proc Natl Acad Sci USA*. 107:14899–14902.